Band Diagram and Effects of the KSCN Treatment in TiO_2/Sb_2S_3/CuSCN ETA Cells

Supporting Information

Yafit Itzhaik,[1] Tatyana Bendikov,[2] Douglas Hines,[3†] Prashant V. Kamat,[3] Hagai Cohen,[2]* and Gary Hodes[1]*

[1] Department of Materials and Interfaces and [2] Department of Chemical Research Support, Weizmann Institute of Science, Rehovot, 76100, Israel

[3] Department of Chemistry and Biochemistry, University of Notre Dame, Notre Dame, Indiana 46556, USA

[†] Present address: Lycoming College, 700 College Place, Williamsport, PA 17701

*Corresponding authors: gary.hodes@weizmann.ac.il, hagai.cohen@weizmann.ac.il

1. CuSCN layer properties

The presence of the α-CuSCN phase in KSCN-treated CuSCN layer was investigated by analyzing varying thicknesses (by varying the deposition volume) of CuSCN on TiO_2/In-OH-S/Sb_2S_3 cells in XRD. By this method it was found that α-CuSCN diffraction peaks appeared already for very thin KSCN-treated CuSCN layers, i.e. inside the pores of the sample. The α-CuSCN peaks intensified significantly with time in both thin CuSCN layers and overlayers, together with a decrease in the β-CuSCN peak intensity, indicating that the CuSCN recrystallizes with aging inside the pores and in the overlayer (Fig S1).

Similar analysis of untreated CuSCN layers of varying thicknesses found no indication of α-CuSCN phase either inside the pores of the cell or in the overlayer, showing the β-CuSCN phase only in all cases.

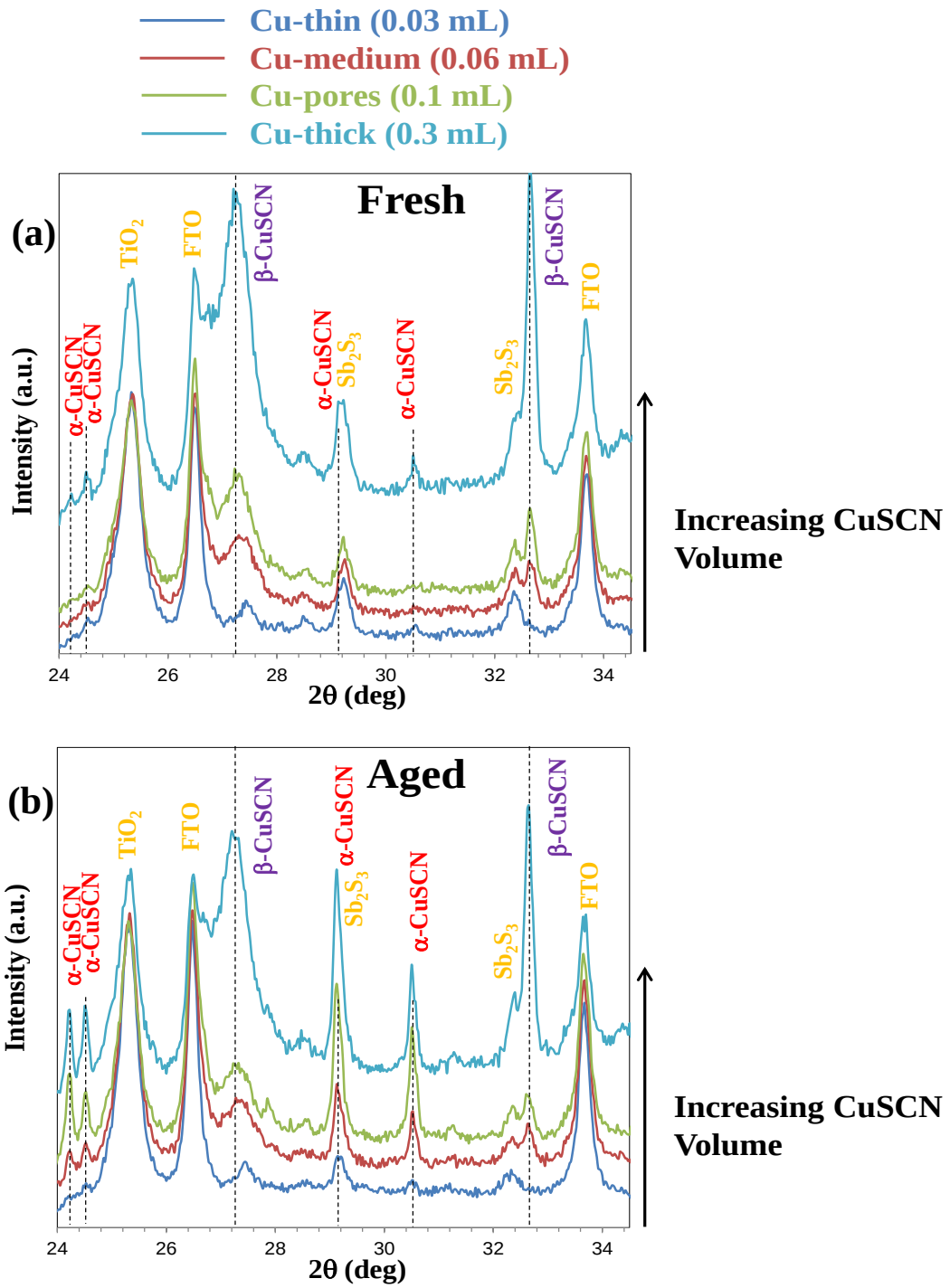

Figure S1. The crystal growth of CuSCN in KSCN-treated Sb_2S_3 cells at various stages of CuSCN deposition (by different added volume (X mL), starting from thin CuSCN layers (Cu-thin and Cu-medium), filling all the pores (Cu-pores), and forming an overlayer on top of the porous matrix (Cu-thick)): (a) fresh samples, measured in XRD right after CuSCN deposition. (b) The same samples after 2 months of aging (stored in a desiccator under low vacuum).

2. XPS characterization of CuSCN inside the pores

We compare the crystallite distribution of the CuSCN inside the pores of the TiO_2/In-OH-S/Sb_2S_3 matrix with the KSCN treatment and without by examining the XPS data of the underlying components (all observable elements are quantified in this full analysis). First, we investigate Cu/Sb atomic concentration ratio: For the thin CuSCN samples, the Cu/Sb atomic concentration ratio in the KSCN-treated samples is ca. 2 times higher than in the untreated one (Table S1). That in itself is clear indication that the deposition of the CuSCN is preferential to Sb_2S_3 sites when the KSCN treatment is employed (higher interface between Sb_2S_3 and CuSCN). This observation is further supported by examining the respective Sb/Ti atomic ratio: If the KSCN-treated CuSCN is deposited preferentially on Sb_2S_3 domains, we expect a decrease in the Sb/Ti ratio in comparison to untreated samples, as indeed occurs (Table S1).

Atomic concentration ratio	KSCN-treated cell	Untreated cell
Cu/Sb	0.32	0.18
Sb/Ti	0.66	0.84

Table S1. Cu/Sb and Sb/Ti atomic concentration ratios of the KSCN-treated and untreated thin CuSCN layers, deposited on the TiO_2/In-OH-S/Sb_2S_3 film.

3. Energy band alignment of Sb_2S_3 cells

The band diagrams in Fig. 6 of the main text show the energy band offsets at their final stage in the cell construction. Here we describe a more realistic potential profile, representing the measured points across both the TiO_2/Sb_2S_3 and the Sb_2S_3/CuSCN junctions (Fig. S2) of the KSCN-treated[1] and untreated cells. As illustrated in Fig. S2, the red dots depict measured data points, whereas the full curves are an educated guess. The difference in the measured data points (in particular the TiO_2 data) between the two sets of experiments is partially due to variations in cell fabrication techniques during the time elapsed between the measurements, which introduced variations in cell components, and therefore affected the electrically-sensitive CREM data. In particular, it is stressed that the difference between top and bottom diagrams

at the back side of the titania, 180 meV in work function, is ***not*** related to the KSCN treatment, but to changes (mainly different sources of reagents) in sample preparation. Yet, consistency within each set of samples (the treated as well as the untreated set) was retained. Thus, we could show how the early stages of CuSCN deposition on a KSCN-treated surface give rise to significant band-bending at the top Sb_2S_3/CuSCN junction as well as the inner TiO_2/Sb_2S_3 junction,[1] whereas CuSCN deposition on the untreated surface does *not* induce band-bending at all, neither at the top junction nor at the inner one. Moreover, by gradually increasing the CuSCN amount, we could show how the top of the valence band position shifts significantly in the untreated cell, whereas for the KSCN-treated cell it undergoes slight changes only (see Fig. 6 in main text). Both the latter observations reflect the creation of a depletion layer when the KSCN treatment is not applied.

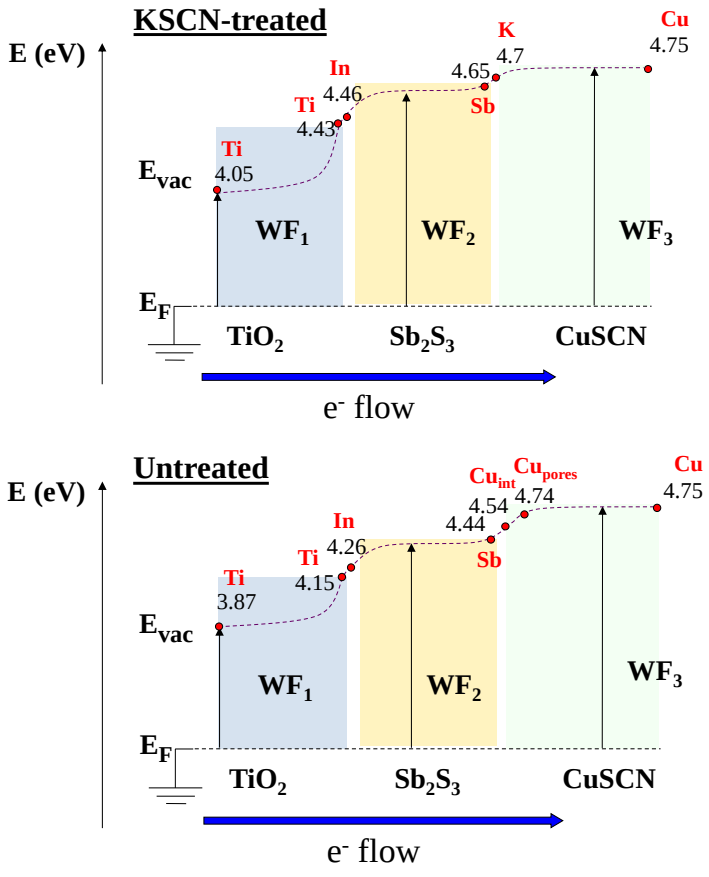

Figure S2. Schematic diagrams representing the final potential profile across the double junction of the cell (after contact) in KSCN-treated (top, adapted from ref. 1) and

untreated (bottom) cells. The curves (broken lines) connecting measured data points (red dots) are guesses and may deviate from the real potential profile. This is particularly so for the field in the TiO_2, where we have little idea at present of the real profile shape. Note the differences between the two cells across the upper junction (see discussion including the comment on the TiO_2 back-side).

We can estimate maximum values of V_{OC} (at saturation light intensity) based on the band diagrams using two different criteria. Based on the built-in fields in the potential profile (measured from the differences in E_{vac}), the maximum V_{OC} is 880 mV for untreated cell and 700 mV for treated one.[2] Ignoring fields and considering band offsets between the Sb_2S_3 CB and that of the TiO_2, and the same for the Sb_2S_3 VB and that of the CuSCN (see Fig. 6 in main text), we arrive at 970 mV for the untreated cell and ~1.00 V for the treated one. Again, these interpretations from the band diagrams cannot explain the higher V_{OC} from the KSCN-treated cell. From the I-V measurements of untreated Sb_2S_3 cells, all cell parameters were significantly lower than the KSCN-treated cell and, in particular, the V_{OC} values of untreated devices do not exceed 450 mV, while in the KSCN-treated cells the V_{OC} reaches reasonable values of 520-560 mV range. These observations give further support to the hypothesis that the main energy loss in the untreated cells is due to the depletion layer forming at the Sb_2S_3/CuSCN interface.

4. The Sb_2O_3 layer

According to the XPS chemical analysis, the Sb_2O_3 is already present in the as-deposited film, and can be spectrally resolved from the Sb_2S_3 component (Fig. S3 top). After annealing, the Sb_2O_3 becomes the more dominant signal (Fig. S3 bottom), indicating that an oxide layer forms on top of the Sb_2S_3 grains.

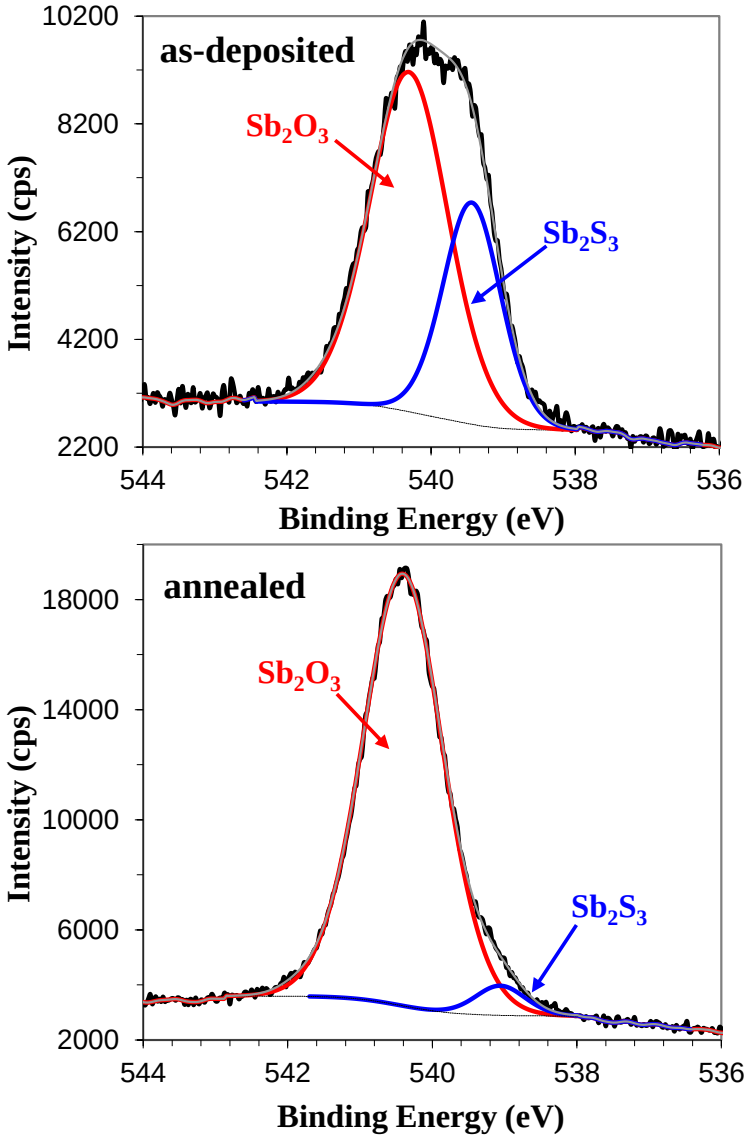

Figure S3. Sb $3d_{3/2}$ XPS spectra of the as-deposited (top) and annealed (bottom) Sb_2S_3 film on TiO_2/In-OH-S substrate. The Sb signal is composed of both Sb_2S_3 and Sb_2O_3 components.

5. I-V performance of Sb_2S_3 cells

The results of the post-treatment, followed by annealing and aging on the initially untreated cell performance, as was presented in Fig. 8 in main text, are summed up in Table S2.

Cell	Treatments	V_{OC} (mV)	J_{SC} (mA/cm^2)	FF	Efficiency (%)
(1) KSCN-treated cell	Aged for ca. 2 months	550	9.2	0.42	2.1
(2) Untreated cell	Aged for ca. 2 months, before procedures	450	4.8	0.29	0.6
	after KSCN post-treatment	480	6.0	0.32	0.9
	after annealing at 100 °C	500	6.9	0.35	1.2
	after aging of a few days	510	7.5	0.38	1.4

Table S2. I-V measurements of the KSCN-treated (1) and untreated (2) Sb_2S_3 cells shown in Fig. 8 in main text. Cell area is 1.1 cm^2, measured with a black mask of the same area.

References

(1) Itzhaik, Y.; Hodes, G.; Cohen, H. Band Alignment and Internal Field Mapping in Solar Cells. *J. Phys. Chem. Lett.* **2011**, *2*, 2872–2876.

(2) The potential value at the back end of Fig. S2, corresponding to the TiO_2/FTO interface, is determined at high accuracy from the bare titania surface, using CREM. Possible capacitive contributions at the back contact and the interface itself were thus found to be small and of a sign opposite to that of the device junction fields discussed above. On the other hand, details of the potential drop across the granular TiO_2 layer (e.g., its characteristic length compared with the single grain-size) are as yet unknown.